ISBN: 978-3-95450-208-0 doi:10.18429/JACoW-IPAC2019-WEPMP049

SIMULATIONS OF BEAM SHAPING FOR DARK MATTER EXPERIMENTS AT LCLS-II*

Y. Nosochkov†, C. Hast, T.W. Markiewicz, L.Y. Nicolas, T.O. Raubenheimer, M. Santana-Leitner
SLAC National Accelerator Laboratory, Menlo Park, CA, USA

Abstract

A new transfer beamline, called S30XL, and an experimental facility are proposed to be built at SLAC, taking advantage of the LCLS-II free electron laser (FEL) under construction. The S30XL will operate parasitically to the FEL by extracting the unused low intensity 4-GeV LCLS-II bunches into the existing A-line and the End Station-A (ESA). This provides a unique capability of multi-GeV nearly continuous electron beam for a variety of HEP experiments, in particular the dark matter search experiments. The latter require a very low beam current ranging from pA to μA, as well as a large beam spot at the detector. The necessary beam shaping will be performed using spoilers and collimators in the A-line, and by optimizing the optics. FLUKA and `elegant` codes are used to generate and track the beam into the ESA.

INTRODUCTION

Construction of the LCLS-II [1] free electron laser (FEL) at SLAC presents a cost-effective opportunity for a variety of HEP applications including dark matter search experiments. High-rate electron beams from the LCLS-II 4-GeV superconducting linac (with a possibility of 8-GeV upgrade) are well suited for this purpose. S30XL (formerly DASEL [2]) is a beamline and detector facility proposed to be built to host such experiments. Two detector proposals, LDMX [3,4] and SuperHPS [5,6], are being developed. These experiments require very low beam charge as well as a large beam spot at the detector. This beamline directly addresses Priority Research Direction 1 of the recent DOE Basic Research Needs workshop [7].

The S30XL is designed to operate parasitically to the FEL. The S30XL beamline connects the LCLS-II with the existing A-line. A fast S30XL kicker placed downstream of the FEL kickers extracts "dark current" bunches from the RF gun or low charge bunches intentionally generated using a 46-MHz laser at the gun. This beam is transported through the S30XL beamline into the existing A-line and to the End Station-A (ESA), where the experiments will take place. Beam parameters in the accelerator and beam specifications for the LDMX are shown in Table 1.

Adjustment of the bunch charge and the transverse beam size (shaping) will be performed using spoilers and collimators in the A-line. This method has been demonstrated in the End Station Test Beam project (ESTB) [8], where a low charge beam is generated by steering selected LCLS [9] bunches onto a Cu-target upstream of the A-line. The scattered electrons with a wide energy spread are then transported through the A-line into ESA. Spoilers and collimators in the A-line are used to control the beam charge and geometrical acceptance. Delivery of individual electrons per pulse and a factor of 10^4 reduction in energy spread had been demonstrated.

Table 1: Beam Parameters in Accelerator, and Beam Specifications for the LDMX Experiment in ESA

Parameter	Accelerator	ESA (LDMX)
Energy	4 GeV	4 GeV
Bunch spacing	5.4-21.5 ns	5.4-21.5 ns
Beam current	<25 nA	0.1 – 150 pA
Bunch charge	<3350 e-	0.015 – 20 e-
Transmission	1	$5{\cdot}10^{-6}$ – $6{\cdot}10^{-3}$
Norm. emittance	1 – 25 μm	$<10^4$ μm
Energy spread	<2%	<1%
Spot size	–	~ 4 × 4 cm^2
Maximum power	55 W	0.5 W

OPTICS

Nominal optics of the S30XL beamline and the A-line is shown in Fig. 1. Locations of the aluminum spoiler PR10 and the momentum slit SL10, used for beam shaping in this study, are indicated by the red lines.

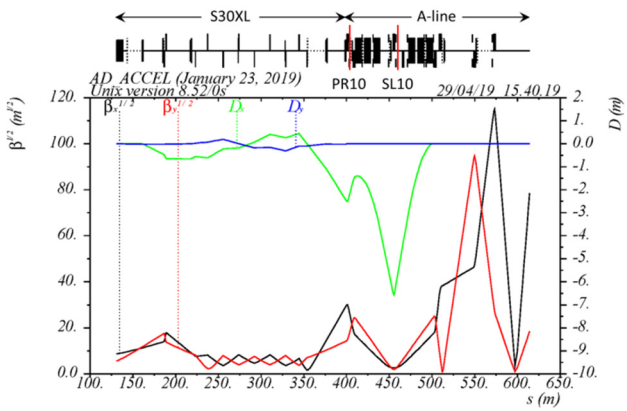

Figure 1: Nominal optics functions of S30XL and A-line, also showing locations of PR10 and SL10 (red bars).

The S30XL beamline consists of a fast kicker, horizontal septum magnet, three dipoles and 14 quadrupoles which are compatible with 8 GeV. The A-line contains twelve strong horizontal dipoles with a total bending angle of 24°, and eight quadrupoles. For this study, we add two quadrupoles in the ESA, where the detector will be located. A notable feature is a very large dispersion at center of the A-line bending system, where the momentum slit SL10 is located. The 6-m dispersion creates a large horizontal spread of the electrons with different energies; this allows to extract electrons with desired energy by using a sufficiently small horizontal aperture of the SL10.

* Work supported by the U.S. DOE Contract DE-AC02-76SF00515.
† yuri@slac.stanford.edu

ISBN: 978-3-95450-208-0 doi:10.18429/JACoW-IPAC2019-WEPMP049

BEAM

In this study, we simulate the process of reducing the incoming beam charge to the level specified in Table 1 and its transport to the ESA. The initial 4 GeV Gaussian beam contains $2{\cdot}10^5$ electrons with rms normalized emittance of 1 μm and 0.5% rms energy spread. This beam is impinged on an aluminium spoiler PR10 upstream of the A-line dipoles. The resulting spoiled beam, generated by FLUKA [10,11], has large energy spread, emittance, and angular divergence – see Fig. 2. Optics functions are also changed. The resulting electron density is reduced, thus helping to extract smaller number of electrons through the SL10 aperture. Two options of the PR10 thickness are tried: 500 μm and 50 μm. The number of generated secondary particles is negligible in these cases.

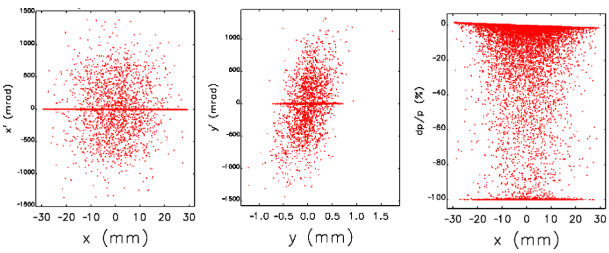

Figure 2: Beam phase space after 500 μm thick aluminum PR10 spoiler: X-X′ (left), Y-Y′ (center), X-Δp/p (right).

The spoiled beam is transported through the first six A-line dipoles and two quadrupoles to the SL10, where it is collimated to the desired bunch charge. The SL10 is a water cooled aluminum collimator, capable of absorbing up to 2 MW of beam power. Its horizontal jaws provide as small as ±50 μm horizontal aperture. The latter is centered on the beam nominal trajectory, so only the electrons near X = 0 can pass through.

In order to achieve a low beam charge after SL10, we transmit a slice of lower energy electrons of the spoiled beam where density is reduced. To do so, we set the magnet field to the desired energy (E), so these electrons follow the nominal orbit, while the nominal energy (E_0) beam core exhibits an orbit proportional to dispersion and $\delta = (E_0 - E)/E$. To avoid large losses, the beam core orbit must be within the magnet aperture. Due to the large dispersion, this limits the minimum slice energy to about 3.96 GeV. Quadrupole strengths are optimized for minimal size of the beam core. In the study, we compare options of 3.97 GeV and 3.98 GeV electron transmission. An example of the 4 GeV beam core orbit between PR10 and SL10 is shown in Fig. 3, where the field is set for 3.97 GeV. Here, the beam core is offset by 35 mm from the SL10 center, hence it is stopped at the SL10.

The off-energy electrons to be transmitted have initial orbit due to the initial dispersion at PR10. This orbit could prevent a clean transmission through the SL10. To cancel this orbit, trim correctors are introduced in the first and sixth dipoles. Example of corrected orbit of 3.97 GeV electrons is shown in Fig. 4. Finally, optics functions downstream of the SL10 for the selected energy electrons are optimized for minimal beam size to minimize losses. Two quadrupoles are added in the ESA to provide flexibility for beam spot adjustment at the detector. Example of analytic 3σ beam size for 3.97 GeV electrons after optimization is shown in Fig. 5 for 500 μm PR10.

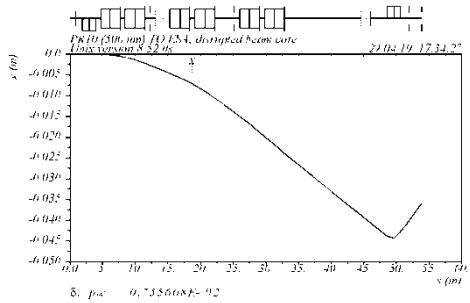

Figure 3: X-orbit of 4 GeV beam core from 500 μm PR10 to SL10, where magnet field is set for 3.97 GeV.

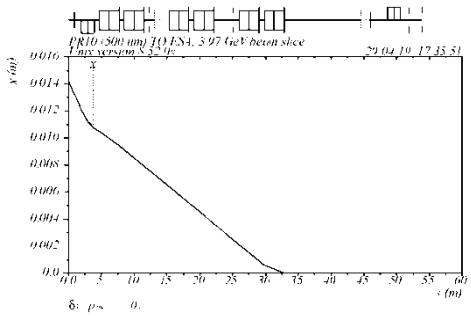

Figure 4: X-orbit of 3.97 GeV electrons from PR10 to SL10 after correction.

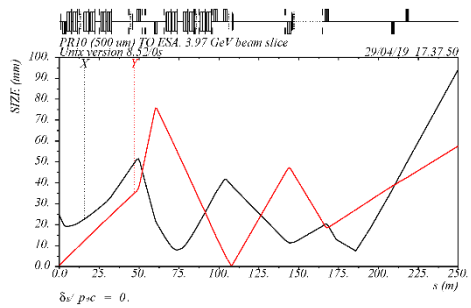

Figure 5: Optimized 3σ size of 3.97 GeV electrons from 500 μm PR10 to ESA.

TRACKING

The beam is tracked from the PR10 spoiler to the ESA using `elegant` code [12] for two options of the PR10 thickness (500 μm and 50 μm) and two options of the transmitted energy (3.97 GeV and 3.98 GeV). A thicker PR10 creates a larger beam spread helping to reduce the electron density in the extracted energy slice, while a thinner PR10 reduces beam losses due to the smaller emittance. At lower extracted energy, the number of electrons to be transmitted is reduced, but the beam core losses are increased due to larger δ.

In the region from PR10 to SL10 the most losses occur due to the large energy spread and dispersion. These losses reduce the initial 100% energy spread at PR10 to ±2% at the SL10 entrance – see Fig. 6, where black lines indi-

ISBN: 978-3-95450-208-0 doi:10.18429/JACoW-IPAC2019-WEPMP049

cate the energy slice to be transmitted through the small SL10 aperture. The 4 GeV beam core is horizontally offset at the SL10 and hence stopped there.

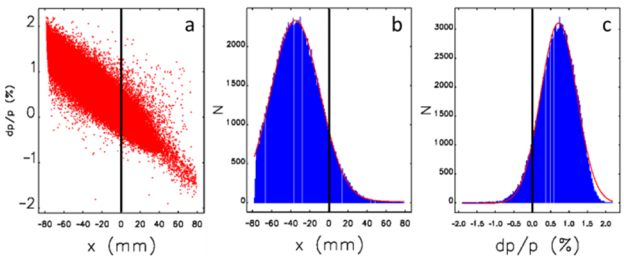

Figure 6: X-Δp/p beam spread at SL10 entrance for the case of 500 μm PR10. Black lines indicate the 3.97 GeV slice to be extracted through small aperture of SL10.

Beam transmission rate in magnets upstream of the SL10 is shown in Fig. 7. The higher loss in case of 500 μm PR10 is due to the larger energy spread. The most loss occurs in the Q19 quadrupole with the largest dispersion. The higher loss at 3.97 GeV is due to the beam core loss since it has a larger δ-offset relative to this energy slice. For the 55-W beam, these losses are acceptable.

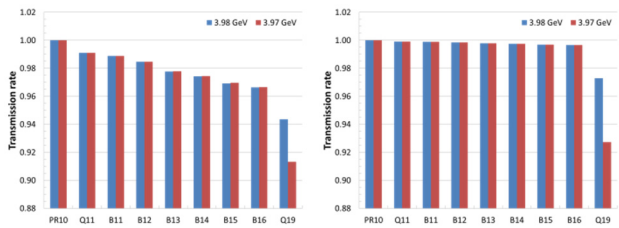

Figure 7: Transmission rate from PR10 to SL10 for 500 μm PR10 (left) and 50 μm PR10 (right), where the magnet field is set for 3.98 GeV or 3.97 GeV.

For the existing SL10 with the smallest horizontal aperture of ±50 μm, the beam after SL10 is shown in Fig. 8. The vertical spread remains large, and the energy spread is influenced by large amplitude electrons due to large emittance. Transmission rate to the ESA vs the SL10 horizontal aperture is shown in Fig. 9. The rate is similar for the 500 μm and 50 μm PR10. The 3.97 GeV option yields a lower bunch charge. However, even at this small SL10 aperture the rate is >$6{\cdot}10^{-4}$, hence more collimation is required to reach the specifications in Table 1.

Other existing collimators in the A-line could be used to further reduce the transmission rate. For this study, instead, we add a vertical collimator SL10Y immediately after the SL10. Figure 10 shows the transmission rate vs the SL10Y aperture where the SL10 X-aperture is ±50 μm. The 500 μm PR10 yields a lower rate reaching the required level of $5{\cdot}10^{-6}$ at the Y-aperture of ±250 μm, while the 50 μm PR10 beam needs much tighter collimation due to the smaller emittance. The lower energy option is preferred for the lowest transmission rate.

Finally, sensitivity to the incoming beam orbit is evaluated assuming ±2% field error of the S30XL vertical kicker. It causes ±1.1 mm vertical offset and ±77 μrad vertical angle at the PR10. Adding these systematic errors to the spoiled beam coordinates alters the transmission rate by ~5% when the rate is 10^{-3}, and a factor of 2 if the rate is ~10^{-5}. In the latter case, the large effect is due to low statistics where only a few electrons out of $2{\cdot}10^5$ are transmitted. The impact of the kicker error is lessened due to the nearly 3π phase advance from the kicker to the SL10. In operation, the collimator apertures and the rate will be experimentally determined.

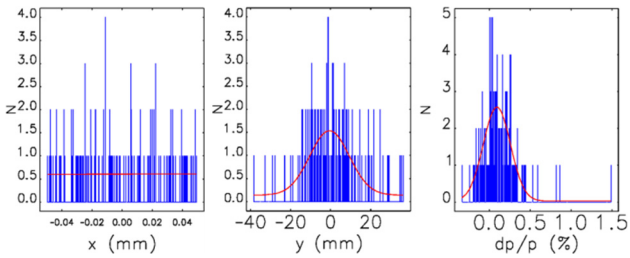

Figure 8: X (left), Y (center), and Δp/p (right) distribution of 3.97 GeV electrons after SL10 with ±50 μm X-aperture and large Y-aperture for the case of 500 μm PR10.

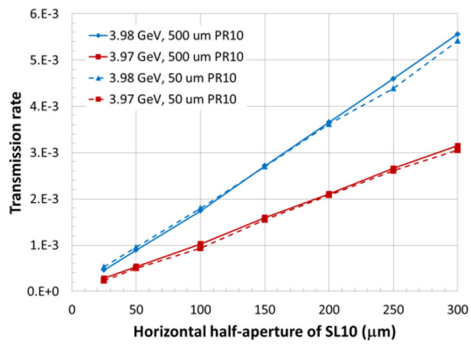

Figure 9: Transmission rate to ESA vs SL10 X-aperture for 3.98 GeV and 3.97 GeV electrons, and 500 μm and 50 μm PR10, where SL10 Y-aperture is large.

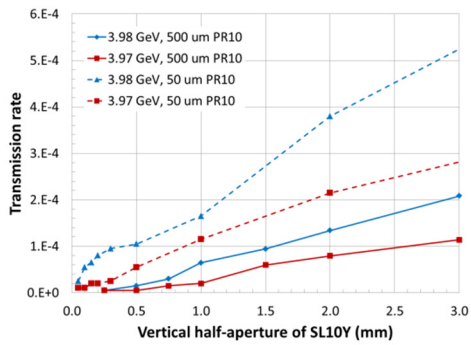

Figure 10: Transmission rate to ESA vs SL10Y aperture for 3.98 GeV and 3.97 GeV electrons, and 500 μm and 50 μm PR10, where SL10 X-aperture is ±50 μm.

CONCLUSION

As low as $5{\cdot}10^{-6}$ bunch charge transmission rate, required for the S30XL dark matter experiments, is achieved by optimizing the A-line optics and extraction of low energy electrons by means of a spoiler and horizontal

ISBN: 978-3-95450-208-0 doi:10.18429/JACoW-IPAC2019-WEPMP049

and vertical collimators. The rate is sufficiently stable with the expected incoming orbit errors.

REFERENCES

[1] T.O. Raubenheimer, "LCLS-II: status of the CW X-ray FEL upgrade to the SLAC LCLS facility," in *Proc. 37th International Free Electron Laser Conference (FEL'2015)*, Daejeon, Korea, Aug. 2015, paper WEP014, pp. 618-624.

[2] T. Raubenheimer et al., "DASEL: Dark Sector Experiments at LCLS-II," SLAC-PUB-17225, arXiv:1801.07867 (2018).

[3] E. Izaguirre, G. Krnjaic, P. Schuster, and N. Toro, "Testing GeV-scale dark matter with fixed-target missing momentum experiments," PRD91 (2015) 9, 094026, arXiv:1411.1404 [hep-ph].

[4] T. Nelson, "Light Dark Matter eXperiment: a missing momentum search for light dark matter," in *US Cosmic Visions: New Ideas in Dark Matter Workshop*, University of Maryland, College Park, USA, Mar. 2017, https://indico.fnal.gov/conferenceDisplay.py?ovw=True&confId=13702

[5] M. Graham, T. Maruyama, and T. Nelson, "Thoughts on future Heavy Photon Searches," in *Snowmass on the Mississippi Workshop (CSS'2013)*, University of Minnesota, Minnesota, USA, Jul. 2013, https://indico.fnal.gov/contributionDisplay.py?contribId=422&confId=6890

[6] M. Graham, "Extending the reach in an HPS-style experiment," in *Snowmass on the Mississippi Workshop (CSS'2013)*, University of Minnesota, Minnesota, USA, Jul 2013, https://indico.fnal.gov/contributionDisplay.py?contribId=423&confId=6890

[7] DOE HEP Workshop on Basic Research Needs for Dark Matter, Small Projects, New Initiatives, 2018, https://science.energy.gov/~/media/hep/pdf/Reports/Dark_Matter_New_Initiatives_rpt.pdf

[8] H. Fieguth et al., "ESTB: A New Beam Test Facility at SLAC," In *Proc. 2nd International Particle Accelerator Conference (IPAC 2011)*, San Sebastian, Spain, Sep. 2011, paper WEPZ017, pp. 2808-2810.

[9] P. Emma et al., "First lasing and operation of an angstromwavelength free-electron laser," Nature Photonics, vol. 4, pp. 641-647, Aug. 2010.

[10] G. Battistoni *et al.*, "Overview of the FLUKA code," Annals of Nuclear Energy 82, 10-18 (2015).

[11] A. Ferrari, P.R. Sala, A. Fasso, and J. Ranft, "FLUKA: a multi-particle transport code," CERN-2005-10, INFN/TC_05/11, SLAC-R-773 (2005).

[12] M. Borland, "elegant: A Flexible SDDS-Compliant Code for Accelerator Simulation," Advanced Photon Source LS-287 (2000).